3-D Finite Element Modeling and Validation of Power Frequency Multi-Shielding Effect

Z.Cheng, N.Takahashi[1], B.Forghani[2], L.Liu, Y.Fan, T.Liu, J.Zhang, and X.Wang

R & D Center, Tianwei Group Co., LTD, Tianwei West Road No. 2399, Baoding 071056, CHINA
[1]Dept. of E.E., Okayama University, Okayama 700-8530, JAPAN
[2]Infolytica Corporation, Montreal, QC H2X 4B3, CANADA
E-mails: emlabzcheng@yahoo.com; [1]norio@elec.okayama-u.ac.jp; [2]forghani@infolytica.com

Abstract — The electromagnetic screen and the magnetic shunt or a combination of the two are widely used in electrical devices in order to control the stray-field and reduce the power loss that may lead to hazardous local overheating. This paper focuses on the 3D finite element modeling of the power frequency inter-shielding effect, the corresponding power loss evaluation, and the validation based on the benchmark shielding models.

I. Introduction

In very large electromagnetic devices, the reduction of stray-field loss and the protection from unallowable loss concentration have become more and more significant. Various types of power frequency shields, including the electro-magnetic screen and the magnetic shunt, or a combination of two are widely utilized to effectively save energy and ensure a reliable operation [1,2]. In addition, the shields can change and control the global distribution of the 3-D electromagnetic field within a large device. It is important to accurately model the inter-shielding effect and optimize the complex shielding configuration at the electromagnetic design stage and not use a rough estimation.

The purpose of this paper is to investigate the inter-shielding effect of the low frequency shields and predict the global distribution and local concentration of power loss under different shielding configurations for different excitations.

II. Shielding Configurations

Three kinds of shielding models, called CS1 to CS3, are prototyped based on the TEAM Problem 21, in which the twin exciting-coil is a stray-field generator working at different excitations. The exciting currents can range from 10 to 25A (50Hz) and flow in 180° phase-angle difference (type I) or in phase (type II). The test models and the 2-D magnetic field distributions are shown in Figs.1-3.

In models CS1 to CS3, the dimensions of the grain-oriented (GO) silicon steel sheets and the copper plate are the same as those of benchmark models P21^c-M1 and P21^c-EM1[3], but the GO silicon steel sheets 30RGH120 are substituted by 30P120, and the 10 mm thick magnetic steel plate in the original shielding models (P21^c-M1 and P21^c-EM1) is removed. The goal is to examine the shielding effect of the different configurations of the laminated sheets and the copper plate as well as the electromagnetic field behavior of the hybrid shields.

III. FE Models for Loss Analysis

In the loss analysis of the magnetic shunt the additional iron loss ($P_{GO\text{-}a}$) induced by the normal flux must be taken into account, as well as the standard iron loss $P_{GO\text{-}s}$ which is determined based on the iron loss curve (W-B_m) measured under the standard condition where the above-mentioned additional iron loss is not considered. The total power loss (P_t) in the hybrid shields can be calculated by (1),

$$P_t = P_{GO-a} + P_{GO-s} + P_{cu-e} \quad (1)$$

where $P_{cu\text{-}e}$ is the eddy current loss induced in the copper plate. A zoning method is employed in the GO silicon sheet's region, i.e., a thin mesh used in the surface layer and a coarse mesh in the remaining inner bulk region of the finite element model [3,4].

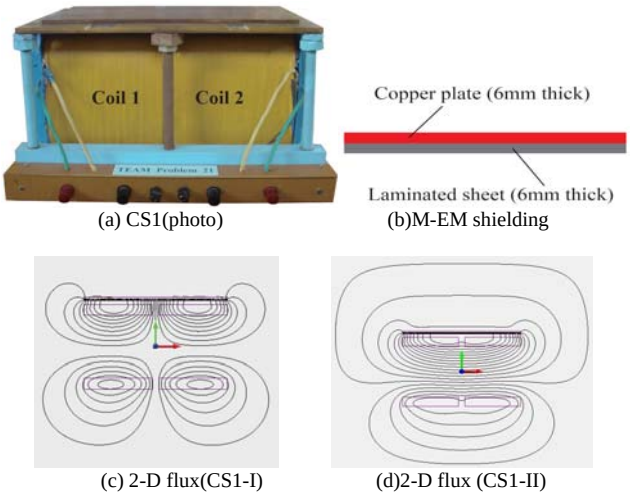

(a) CS1(photo) (b)M-EM shielding

(c) 2-D flux(CS1-I) (d)2-D flux (CS1-II)

Fig.1. Model CS1.

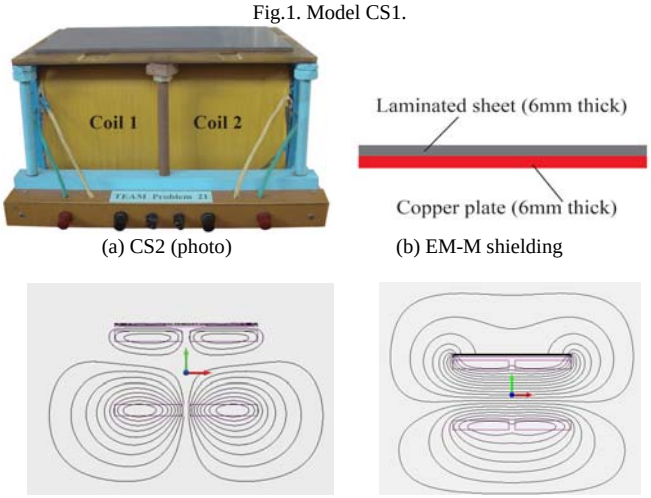

(a) CS2 (photo) (b) EM-M shielding

(c) 2-D flux (CS2-I) (d) 2-D flux (CS2-II)

Fig.2 Model CS2.

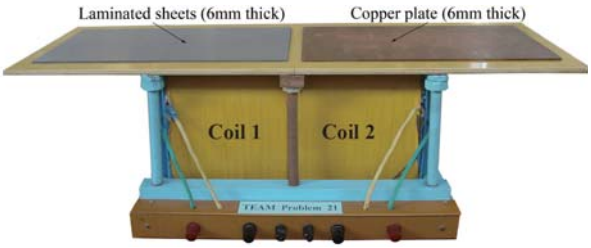

(a) CS3 (photo)

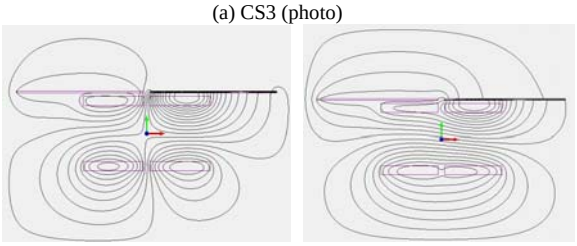

(b) 2-D flux (CS3-I) (c) 2-D flux (CS3-II)

Fig.3. Model CS3.

To further reduce the cost of the electromagnetic field computation in the bulk region, especially for a large-scale laminated core, all the eddy currents induced in the bulk domain are neglected.

It is certainly important to predict the maximum value of the loss density in the shields in order to avoid the impermissible local overheating. The following loss concentration factor C_{loss} is proposed,

$$C_{loss} = \frac{P_{d-\max}}{P_s / V_s} \tag{2}$$

where $P_{d\text{-}max}$ is the maximum loss density (W/m^3) in the magnetic shunt or the electromagnetic screen. P_s and V_s are the total loss (W) and the volume (m^3) of the shielding component.

IV. Results and Discussion

The newly measured (using power analyzer WT-3000, Yokogawa, Japan) and calculated (using MagNet solver, Infolytica, Canada) power losses produced in models CS1 to CS3 at different excitations (i.e., types I and II, and currents ranging from 10 to 25A) are shown in Fig.4.

The loss concentrations inside the shielding components (at 25A), represented by a factor C_{loss}, which must be examined at the EM design stage are shown in Fig.5. The remarkable loss concentration ($C_{loss} \cong 80$) is observed in CS1-I.

The new results for the hybrid shields can be briefly summarized as follows:

1) The calculated and measured loss results for the hybrid shields, which are of quite different mechanism, at different excitations are in good agreement. It is shown that the accurate FE modeling of the shielding effect is practical in the large-scale electromagnetic design.
2) The different stray-field behavior and loss distribution of the different shield configurations can be seen based on the modeling results. In model CS1, the power loss P_{GO} generated in GO sheets is more than 60% of the total power loss P_t at the different excitations; however, in model CS2, the power loss P_{cu}, generated in the copper plate, is more than 98% and P_{cu} is independent of the excitation pattern; in model CS3, the power loss is also concentrated in the copper plate, i.e., P_{cu} is more than 92% of P_t, even though both the laminated GO sheets and the copper plate face the same exciting source. See Table I.
3) Both the total power loss and the loss concentration must be taken into account in the evaluation of the shielding effect from points of view of both energy saving and operational safety.

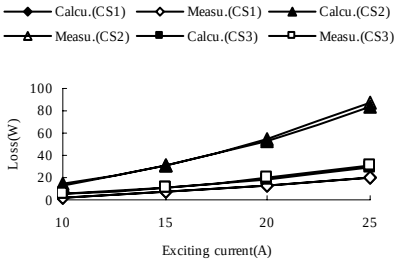

(a) Loss results (type I)

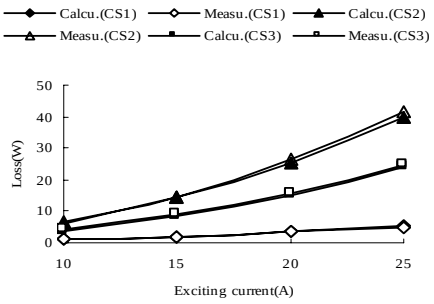

(b) Loss results (type II)

Fig.4 Loss in hybrid shields.

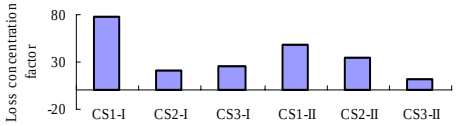

Fig.5 C_{loss} variation with excitation and configuration(25A).

TABLE I
LOSS AND DISTRIBUTED RATIO IN SHIELDING COMPONENTS

Current (A)	CS3-I (W, %,)		CS3-II (W, %,)	
	P_{GO}	P_{cu}	P_{GO}	P_{cu}
10	(0.43) 9.0	(4.28) 91.0	(0.30) 8.0	(3.51) 92.0
15	(0.88) 8.0	(9.64) 92.0	(0.67) 8.0	(7.84) 92.0
20	(1.50) 8.0	(17.11) 92.0	(1.14) 8.0	(13.94) 92.0
25	(2.29) 8.0	(26.73) 92.0	(1.88) 8.0	(21.94) 92.0

V. References

[1] J.Turowski, M.Turowski, and M.Kopec, *IEEE Trans. on Magnetics*, vol. 26, no 5, pp 2911-2919, 1990.

[2] J. Turowski, X.M. Lopez-Fernandez, A. Soto, and D. Souto, Advanced Research Workshop on Transformers, 2007, Spain.

[3] Z.Cheng, N. Takahashi, S. Yang, T. Asano, Q. Hu, S. Gao, X. Ren, H. Yang, L. Liu, and L. Gou, *IEEE Trans. on Magnetics*, vol.42, no.4, pp.1467-1470, 2006.

[4] Z.Cheng, N.Takahashi, B.Forghani, G. Gilbert, Y.Du,Y.Fan, L.Liu, Z.Zhai, W.Wu, and J.Zhang, *IEEE Trans. on Magnetics*, vo.46, no.8, pp.3185-3188, 2010.